ORGANIC CHEMISTRY
FRONTIERS

RESEARCH ARTICLE

Solvent-driven selective π-cation templating in dynamic assembly of interlocked molecules†

Cite this: DOI: 10.1039/c3qo00074e

Andrew B. Pun,[a] Kevin J. Gagnon,[b] Liana Klivansky,[a] Simon J. Teat,[b] Zhan-Ting Li*[c] and Yi Liu*[a]

Received 17th December 2013,
Accepted 14th January 2014

DOI: 10.1039/c3qo00074e

rsc.li/frontiers-organic

Both bispyridinium (**BPY**) and trispyridinium (**TPY**) have been used to template the formation of linear or triply threaded [2]rotaxanes through imine-based dynamic clipping reactions. In this paper, we report contrasting solvent dependence between these two templated clipping reactions when two different solvents, namely $CDCl_3$ and CD_3CN, are used. The solvent dependence is elucidated based on ^1H NMR studies, and structural features are revealed by single crystal X-ray analyses of the respective linear and triply threaded interlocked molecules. We have shown that although both clipping reactions are affected by hydrogen-bonding and aromatic–aromatic interactions in general, the nature of the aromatic–aromatic interactions is quite different, which is responsible for the different solvent response. The **BPY**-based clipping reaction is driven by electrostatic interactions between aromatic surfaces, while the **TPY**-based reaction is mainly governed by the solvation/desolvation effect (solvophobic interactions). These findings led us to design a rare solvent switchable system. In competition clipping experiments employing both **BPY** and **TPY** as the templates, exclusive formation of the **BPY**-based linear [2]rotaxane can be achieved in pure $CDCl_3$, while in pure CD_3CN, a 6.7 : 1 selectivity is achieved in favor of the **TPY**-based triply threaded [2]rotaxane. The detailed structural analysis of the two [2]rotaxanes as well as the solvent-dependent selectivity, may encourage more integrated approaches for the design of complex molecular architectures.

Introduction

Mechanically interlocked molecules,[1] such as [2]rotaxanes and [2]catenanes, first emerged as topologically interesting synthetic targets, and later evolved as the platform for novel molecular,[2] supramolecular,[3] and polymeric materials[4] with unique architectures and functions, which have found many applications in nanomechanical devices,[5] molecular memory,[6] and reconfigurable nanovalves.[7] For the synthesis of [2]rotaxanes, clipping of a macrocycle around a dumbbell-shaped template is one of the most convenient methods[8] as it furnishes the synthesis with minimal steps, higher yields, and product specificity, thanks to the error-checking and self-sorting power endowed by molecular recognition, non-covalent templating and reversible dynamic covalent chemistry (DCC).[9] Among several DCC reactions, the imine chemistry is arguably the most versatile, and has garnered great interest in the assembly of novel structures,[9e,f] including molecular cages,[10] Borromean rings,[11] suitanes,[12] catenanes,[13] rotaxanes,[14] and helixes.[15]

We have been motivated by a π-guest templating protocol for the assembly of C_3-symmetric macrobicycle-based interlocked nanostructures employing dynamic imine chemistry. In this regard, 2-terminal[14c] and 3-terminal [2]rotaxanes[14g] can be obtained in high yields from the reaction between simple precursors such as 1,3,5-benzenetrisaldehyde (**1**) and 2,2′-(ethylenedioxy)diethylamine (**2**) and the respective dumbbell components, such as bipyridinium (**BPY**) or trispyridinium (**TPY**) π-cationic species (Scheme 1). As shown previously by modeling[14c] or single crystal X-ray structures,[14g] the linear [2]rotaxane (**LR**) or the triply-threaded [2]rotaxane (**TR**) are stabilized by favorable aromatic–aromatic interactions between the guest and the C_3-symmetric trisiminophenylene (**TIP**) "ceiling" and "floor". Furthermore, the oligo(ethylene glycol) "pillars" not only provide sufficient flexibility for ideal spacing in between the two **TIP** units (around 7 Å apart between the floor and the ceiling), but also serve as polar binding sites to assist guest encapsulation through multiple [C–H···O] and

[a]The Molecular Foundry, Lawrence Berkeley National Laboratory, One Cyclotron Rd, MS 67R6110, Berkeley, CA 94720, USA. E-mail: yliu@lbl.gov, ztli@fudan.edu.cn
[b]Advanced Light Source, Lawrence Berkeley National Laboratory, One Cyclotron Rd, MS 67R6110, Berkeley, CA 94720, USA
[c]Department of Chemistry, Fudan University, 220 Handan Road, Shanghai 200433, China

† Electronic supplementary information (ESI) available. CCDC 977101–977102. For ESI and crystallographic data in CIF or other electronic format see DOI: 10.1039/c3qo00074e

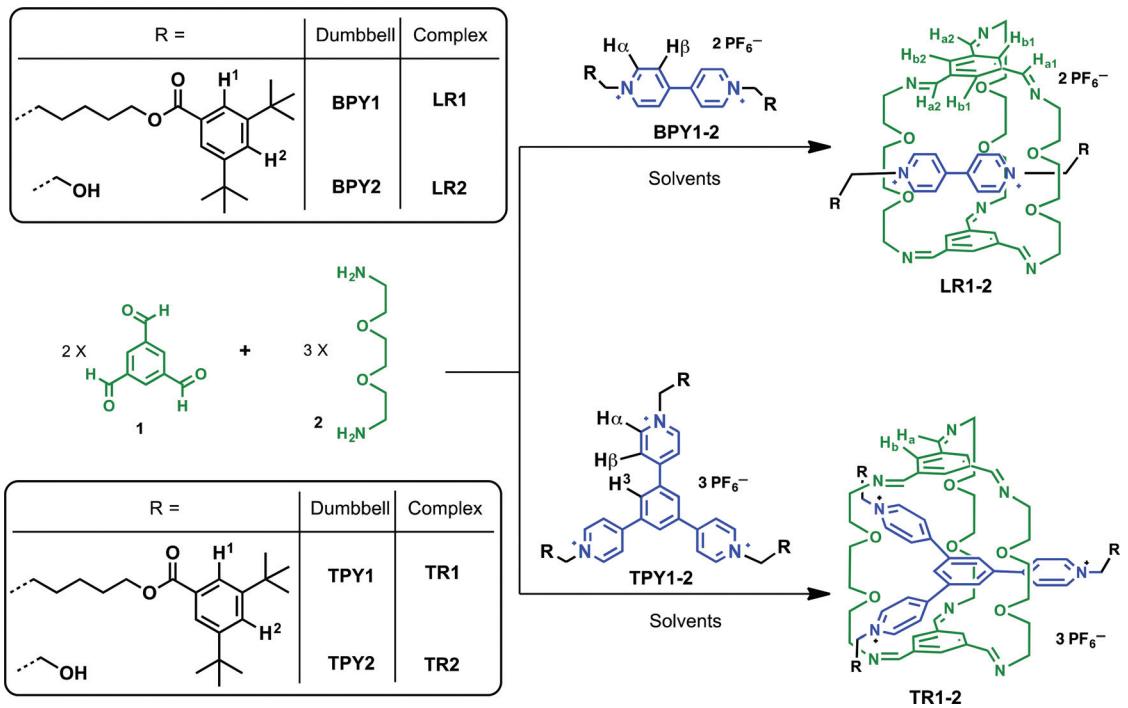

Scheme 1 The clipping reactions of linear (**LR**) and triply threaded [2]rotaxanes (**TR**) from **BPY** and **TPY** guests. Solvents: $CDCl_3$ and/or CD_3CN.

[C–H···N] hydrogen bonding interactions. While the templating capabilities of both linear **BPY** and the triangular **TPY** guests allow us to build complex molecular architectures, more in-depth descriptions of their relative templating power are needed, which are important for answering the following questions: which clipping product is thermodynamically or kinetically favored when both **BPY** and **TPY** are subjected to the clipping reaction? And how do the weak aromatic–aromatic or [C–H···O] interactions respond to the surrounding solvent media? Although there are a few examples of using solvent to drive the conformational selectivity in interlocked molecules,[16] examples of using solvents to affect the selectivity of products in the presence of different templates is rare.[17] In this paper, we report contrasting product selectivity between the **BPY** and the **TPY** templated clipping reactions when two different solvents, namely $CDCl_3$ and CD_3CN, are used. The solvent dependence is elucidated based on ^{1}H NMR studies and structural features are revealed by single crystal X-ray analysis of the respective linear and triply threaded interlocked molecules. We have indicated that although both clipping reactions are affected by hydrogen-bonding and aromatic–aromatic interactions in general, the nature of the aromatic–aromatic interactions is quite different. The **BPY**-based clipping reaction is primarily driven by electrostatic interactions between **BPY** and **TIP** surfaces, while the **TPY**-based reaction is mainly driven by the solvation/desolvation effect (solvophobic interactions). The different solvent responses enable us to construct an unusual solvent-driven switching system between two dynamic [2]rotaxanes in competition experiments.

Experimental details of the clipping reactions

The clipping reactions are conducted by mixing a solution of trisaldehyde **1**, diamine **2** and the corresponding **BPY** or **TPY** guest in a ratio of 2 : 3 : 1 in deuterated solvents unless noted otherwise (Scheme 1). Two different N-substituent groups are employed for both **BPY** and **TPY** compounds. The aliphatic, bulky 3,5-di-*t*-butylbenzoyl ester groups act as stopper units in **BPY1** and **TPY1** while endowing these cationic compounds with good solubility in solvents such as CD_3CN and $CDCl_3$, which is important for following the clipping reactions in single solvent systems. The short ethanol groups in **BPY2** and **TPY2** were introduced in order to facilitate the growth of single crystals of the respective clipping products. In the case of these ethanol derivatives, the optimized solvent systems for conducting the clipping reactions contain a mixture of CD_3CN and $CDCl_3$. It has been found that in pure $CDCl_3$, the limited solubility of the ionic guests precludes the templating from happening, while in pure CD_3CN, oligoimines formed from non-specific condensation have low solubility and quickly precipitate out of the reaction mixture after mixing, resulting in low clipping efficiency. In all cases, the clipping reactions are complete within two hours as monitored by ^{1}H NMR spectroscopy.

When $CDCl_3$ is used as the single solvent for **BPY1** clipping reaction, **LR1** is obtained as the single product, with a significant upfield shift of **BPY** Hα and Hβ resonances in the

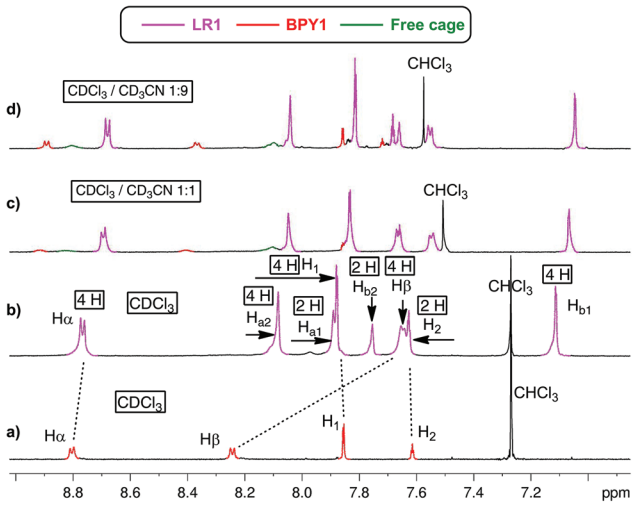

Fig. 1 Partial ^{1}H NMR spectra of (a) **BPY1** in $CDCl_3$, and the clipping reaction based on **BPY1** in (b) $CDCl_3$, (c) $CDCl_3$–CD_3CN (1 : 1, v/v), and (d) $CDCl_3$–CD_3CN (1 : 9, v/v). The resonances are color coded and assigned to the involved species in solution. Purple signals: **LR1**, red signals: **BPY1**, green signals: free cage.

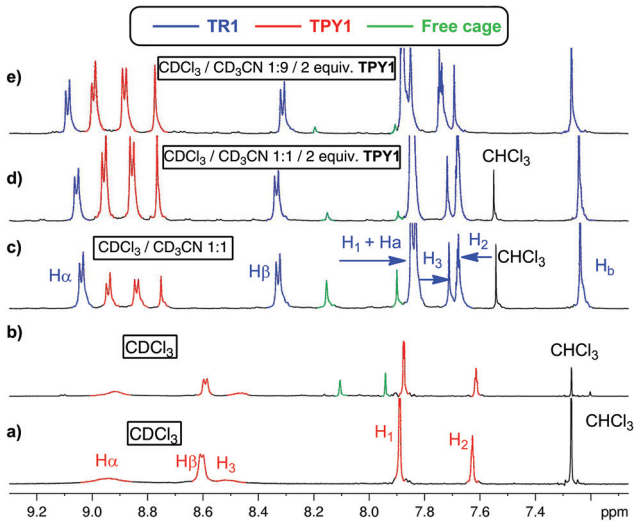

Fig. 2 Partial ^{1}H NMR spectra of (a) **TPY1** in $CDCl_3$, and the **TPY1** based clipping reaction under different conditions. (b) 1 equiv. **TPY1** clipping in $CDCl_3$. (c) 1 equiv. **TPY1** clipping in $CDCl_3$–CD_3CN (3 : 5, v/v). (d) 2 equiv. **TPY1** clipping in $CDCl_3$–CD_3CN (3 : 5, v/v). (e) 2 equiv. **TPY1** clipping in $CDCl_3$–CD_3CN (1 : 9, v/v). The resonances are color coded and assigned to the involved species in solution. Blue signals: **TR1**, red signals: **TPY1**, green signals: free cage.

^{1}H NMR spectrum when compared with that of the free **BPY1** in $CDCl_3$ (Fig. 1a and b). In contrast to the pseudo[2]rotaxane **LR2** that is in fast equilibrium with its components (Fig. S1, ESI†), the macrobicycle in **LR1** is sterically hindered from slipping off the dumbbell and held in place around **BPY1**. Consequently, the symmetry of the macrobicyclic component is lowered so that the six imine protons and six phenylene protons become non-equivalent, each splitting into a set of two singlets in a ratio of 1 : 2. Increasing the amount of CD_3CN to 50% and 90% while maintaining the same sample concentration dissociates **LR1** by 14% and 22%, respectively, as can be seen from the appearance of free **BPY1** and the macrobicyclic cage in the ^{1}H NMR spectra (Fig. 1c and d).

The ^{1}H NMR spectrum of **TPY1** in pure $CDCl_3$ reveals very broad resonances of the central trispyridinium core (Fig. 2a), indicative of dynamic processes in solution. Surprisingly, when **TPY1** is subjected to the clipping reaction in pure $CDCl_3$, there is no [2]rotaxane product, and instead only **TPY1** and the free macrobicyclic cage are observed (Fig. 2b). This is in sharp contrast to the same reaction that is carried out in $CDCl_3$–CD_3CN (3 : 5) (Fig. 2c). A new set of resonances corresponding to the formation of desired **TR1** appears within 10 minutes. Significant quantities of unbound **TPY1** and the free cage are also present in the solution, which, commensurate with the increasing amount of **TR1**, decrease as the reaction progresses and reaches equilibrium after two hours (**TR1** : free cage = 1 : 0.3). Further analysis of the ^{1}H NMR spectrum of the interlocked species **TR1** indicates that the H3 and Hβ resonances in **TPY**, together with the Ha and Hb resonances in **TIP** units, show significant upfield shifting in comparison to those of unbound **TPY1** and the free cage, consistent with a mutual shielding effect between the aromatic units. In contrast, the Hα resonances of **TR1** shift downfield relative to those of unbound **TPY1**, indicating a deshielding effect imposed by the surrounding polyimine aromatic core. Upon addition of 1.0 more equivalents of **TPY1** into the reaction mixture, the equilibrium is further shifted towards nearly complete consumption of the free cage (**TR1** : free cage = 1 : 0.1, Fig. 2d). Increase of the CD_3CN composition to 90% while maintaining the same **TPY1** concentration further decreases the amount of free cage (**TR1** : free cage = 1 : 0.07, Fig. 2e). When this preassembled solution is evaporated and redissolved in $CDCl_3$, the same ^{1}H NMR spectrum as that shown in Fig. 2b is obtained, confirming the complete dissociation of **TR1** in $CDCl_3$.

The contrasting solvent response prompts us to look into the detailed structural features of the respective interlocked assemblies. X-ray quality single crystals were obtained for these interlocked **LR2** and **TR2** using ethanol-derived **BPY2** and **TPY2**.[18] The unit cell of **LR2** contains two crystallographically independent molecules, each comprising nearly parallel stacking of the **BPY** unit and the **TIP** units in the ceiling and the floor of the macrobicycle (Fig. 3). The six imine groups in the cage are coplanar with the conjugating phenylene to give two extended aromatic ring systems, while the **BPY** units in the two crystallographically independent molecules are twisted with dihedral angles of 7.7 and 22.6°, respectively. The distances between the centroids of **TIP** units to the mean plane of **BPY** units are all within 3.23 to 3.38 Å. The conformation is stabilized by multiple [C–H···O] and [C–H···N] hydrogen bonds between (1) two Hαs of the **BPY** unit and the oxygen atoms on the two nearby ethylene glycol loops on the back, (2) two Hβs of the **BPY** unit and two oxygen atoms on the front ethylene glycol loop, (3) methylene protons next to **BPY** and oxygen atoms on the nearby ethylene glycol loops, and (4) one of the

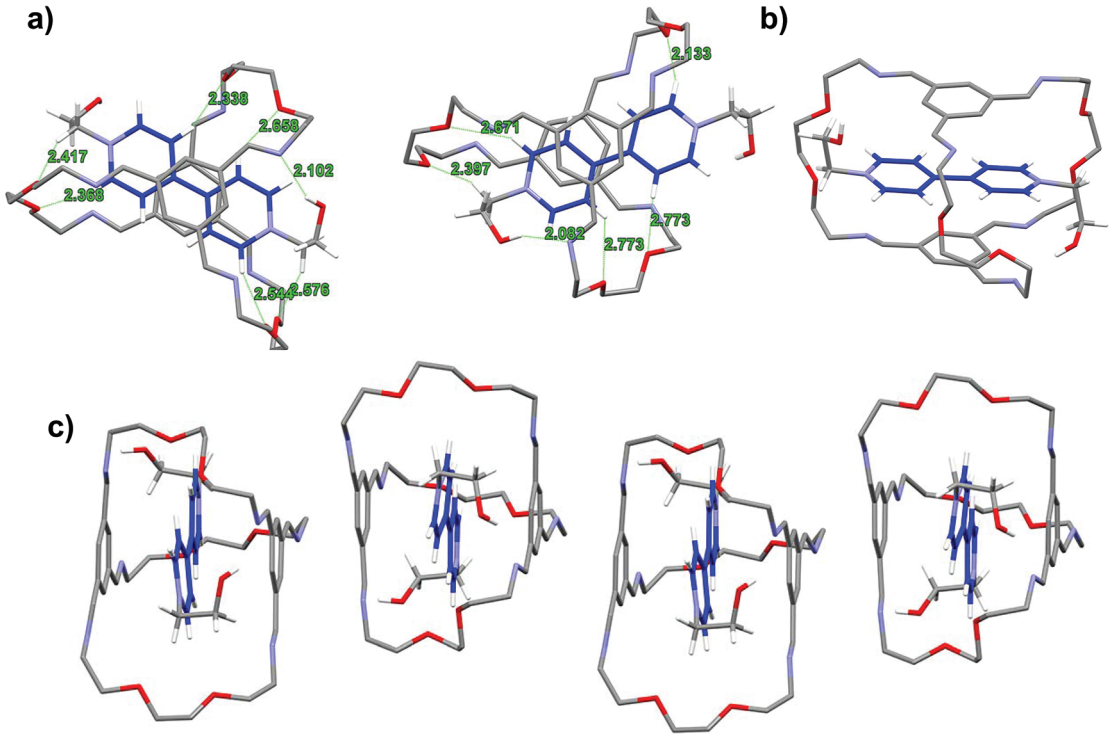

Fig. 3 Capped stick representation of the X-ray structures of **LR2**. (a) Top view of X-ray structure of **LR2** showing two crystallographically independent molecules in the lattice. The green dashed lines indicate [C–H···O] interactions. (b) Side view showing one of the two independent molecules of **LR2**. (c) Elongated π-stacking in the solid state. Solvent molecules, anions and hydrogen atoms on the macrobicycle are omitted for clarity.

hydroxyl protons and one of the C═N nitrogen atoms. In addition, adjacent **LR2** molecules stack into extended π-stacking columns.

In the solid state structure of **TR2** (Fig. 4),[19] the **TPY2** guest is sandwiched within the cavity of the macrobicyclic cage, with the pyridinium arms threading through the three oligo(ethylene glycol) orifices. The two **TIP** units lie nearly parallel with respect to the central phenylene ring in the **TPY** unit with centroid-to-plane distances of 3.50 and 3.48 Å, respectively, which are larger than those in **LR2**. All three pyridinium units of **TPY** are twisted out of the plane of its central benzene ring. The twisting satisfies the desirable geometrical arrangement for multiple [C–H···O] interactions between the oxygen atoms of the oligo(ethylene glycol) units in the cage and four of the Hβs of the three pyridinium units in **TPY**. Additional [C–H···N] and [C–H···O] interactions are also observed between one of the pyridinium Hβ protons and the nitrogen atoms of a **TIB** unit, and between the central phenylene ring in **TPY** and the oxygen atoms of the oligo(ethylene glycol) units, respectively, all of which contribute collectively to the stabilization of the complex. It is worth noting that an uncomplexed **TPY2** guest stacks alongside with the macrobicyclic cage to give a 1 : 2 host–guest complex that extends the π stacking in the solid state.

A comparison of the structures of **LR2** and **TR2** indicates a similar conformation adopted by the macrobicycle; however, the relative positions of pyridinium units within the cavity are significantly different. The pyridinium units in **TPY** extend relatively further out of the cavity because of the central phenylene ring "spacer" and thus have no π-overlap with the **TIP** units on the cage, while those of the **BPY** have more buried π-surfaces that are overlapping with the **TIP** aromatic surfaces. The difference in positioning of the pyridinium units with respect to the macrobicycle also accounts for the different involvement of Hα and Hβs in hydrogen bonding interactions: both Hαs and Hβs in **BPY** are involved in [C–H···O] interactions, while in **TPY**, Hβs and the central phenylene protons are involved but not Hαs, the latter being distant from the hydrogen bonding acceptors on the oligo(ethylene glycol) pillars.

Competition and solvent-induced switching experiments

Encouraged by the opposite solvent responsiveness, we conduct a series of competition and solvent-driven switching experiments (Scheme 2). When equal equivalents of **BPY1** and **TPY1** are mixed and subjected to the clipping reaction in $CDCl_3$, **LR1** is formed exclusively, with free **TPY1** in the solution (Fig. 5a). When equal volume of CD_3CN is added to the mixture, **TR1** started to appear and ended up with a **TR1**/**LR1** ratio of 1.3 : 1 after equilibrium (Fig. 5b). The same distribution of **TR1** and **LR1** is observed when the clipping is conducted in a 1 : 1 mixture of $CDCl_3$ and CD_3CN, excluding any kinetic selection effect and confirming that a thermodynamic

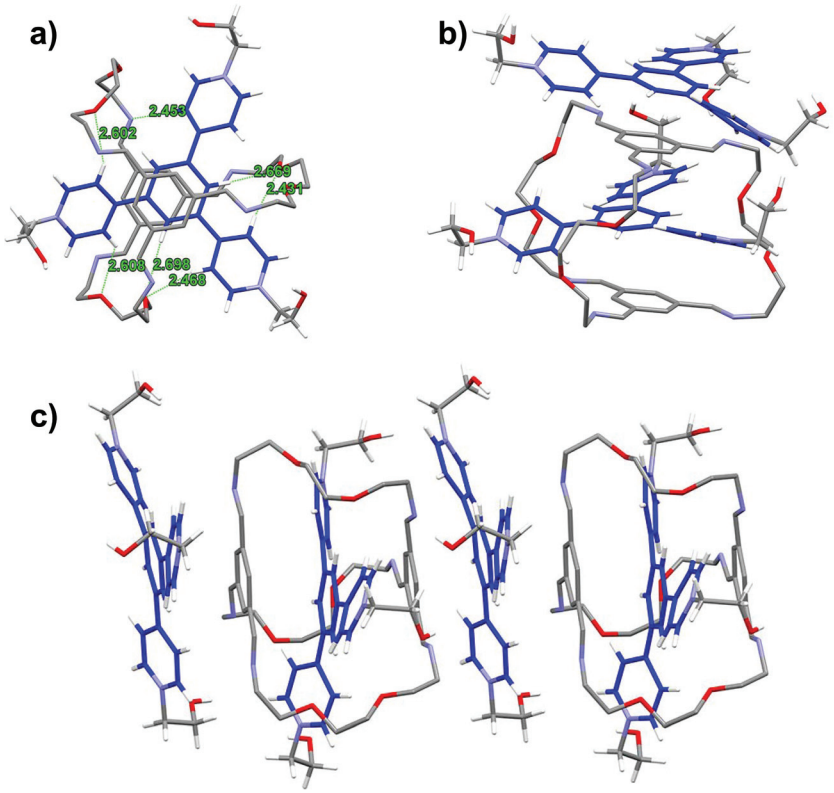

Fig. 4 Capped stick representation of the X-ray structures of **TR2**. (a) Top view of the X-ray structure of **TR2**. The green dashed lines indicate [C–H···O] and [C–H···N] interactions. (b) Side view of the 1 : 2 host–guest complex structure of **TR2**. (c) Elongated π-stacking in the 1 : 2 host–guest complex in the solid state. Solvent molecules, anions and hydrogen atoms on the macrobicycle are omitted for clarity.

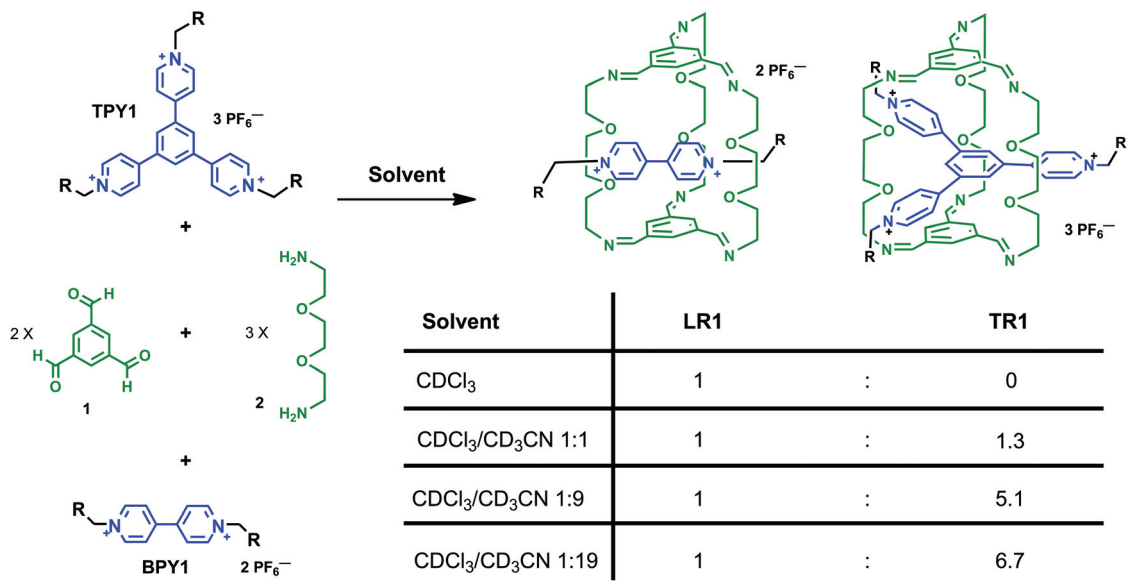

Solvent	LR1		TR1
$CDCl_3$	1	:	0
$CDCl_3/CD_3CN$ 1:1	1	:	1.3
$CDCl_3/CD_3CN$ 1:9	1	:	5.1
$CDCl_3/CD_3CN$ 1:19	1	:	6.7

Scheme 2 Scheme of the competition experiment and the corresponding solvent-dependent selectivity.

equilibrium is reached. Raising the composition of CD_3CN to 90% and 95% increases the **TR1**/**LR1** selectivity to 5.1 : 1 and 6.7 : 1, respectively (Fig. 5c and d). The solvent-dependent selectivity is summarized in Scheme 2.

Discussion of the solvent effect

The main driving interactions involved in these [2]rotaxanes are aromatic–aromatic and hydrogen bonding interactions.

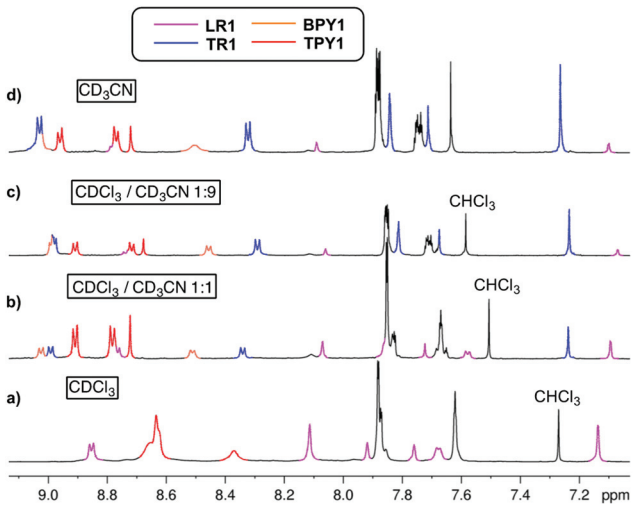

Fig. 5 Competition clipping experiment conducted in (a) $CDCl_3$, (b) $CDCl_3$–CD_3CN (1 : 1), (c) $CDCl_3$–CD_3CN (1 : 9) and (d) $CDCl_3$–CD_3CN (1 : 19). Non-overlapping resonances are color coded and assigned to either the templates or the [2]rotaxanes. Purple signals: **LR1**, blue signals: **TR1**, orange signals: **BPY1**, red signals: **TPY1**.

Polar solvents weaken the hydrogen bonding interactions. For the impact of solvent polarity on aromatic–aromatic interactions, since the nature of such interactions is complementary electrostatic interactions and/or solvation/desolvation effects (*i.e.* solvophobic interactions),[20] the impact is ambipolar: higher polarity weakens electrostatic interactions, and promotes solvophobic interactions in between π surfaces.

For **LR1**, the addition of more polar CD_3CN into $CDCl_3$ decomplexes the interlocked structure, suggesting that the energy gain from aromatic–aromatic interactions, if any, is inadequate to compensate for the destabilized hydrogen bonding interactions. In the case of **TR1**, the solvent response is the opposite. Increasing the composition of CD_3CN in the solvent system favors the formation of **TR1**, while $CDCl_3$ decomplexes the interlocked [2]rotaxane, and in 100% $CDCl_3$ there is no **TR1** despite the fact that it is a more benign solvent for hydrogen bonding. While this suggests that aromatic–aromatic interactions are more dominant than [C–H···O] hydrogen bonding interactions in stabilizing the interlocked structure, there might exist other competing processes that affect the equilibrium, as indicated by the broad ^{1}H NMR resonances of the aromatic core of **TPY1** in $CDCl_3$. Variable temperature experiments are conducted to reveal the temperature dependence of the peak broadening. As shown in Fig. S2 in ESI,† the Hα and H3 resonances of the **TPY1** core are shifted and become broader as the temperature is lowered, and are almost concealed in the baseline as the temperature approaches the melting point of $CDCl_3$. The line broadening implies that the resonances are close to coalescence between equilibrating species, which is presumably a result of self-aggregation of **TPY1** through dimerization/oligomerization. It is postulated that while the lipophilic end groups of **TPY1** ensure good solubility in less polar solvents like $CDCl_3$, the tricationic core of **TPY1** is poorly solvated. Consequently, **TPY1** molecules tend to aggregate with the trispyridinium units congested together to form an inner core with a surrounding outer shell of the alkyl ester end groups. In less polar $CDCl_3$, this aggregation gives the least exposed polar surface area, and is more favored over the formation of interlocked species. In contrast, well-resolved resonances are observed for **TPY1** in the presence of CD_3CN, (Fig. S8 in ESI†) indicating better solvation of the trispyridinium core and insignificant aggregation. In addition, the better yield of **TR1** at higher composition of CD_3CN suggests that while aggregation and [C–H···O] hydrogen bonding interactions become insignificant, aromatic–aromatic interactions are reinforced to compensate for the energy penalty. The different solvent responses can be further discussed on account of the following aspects:

(1) The [C–H···O] hydrogen bonding strength is different. In **BPY1**, both Hα and Hβ-protons are involved in [C–H···O] interactions, while in **TPY1**, only Hβ-protons and the phenylene protons are involved in [C–H···O] interactions, which are much less acidic than Hα and weaker H-bonding donors.

(2) The electron densities of the guest π-surfaces are different. Electrostatic surface potential (ESP) plots indicate (Fig. S3 in ESI†) that both **BPY** and **TPY** aromatic cores are electron deficient while the **TIP** units of the macrobicycle are relatively electron rich. Cyclic voltammetric studies performed in MeCN (Fig. S4 in ESI†) indicate that **BPY1** has a much less negative half-wave reductive potential than **TPY1** ($E_{1/2}$: −0.81 V *vs.* −1.38 V, with reference to F_c/F_c^+), confirming that **BPY1** is a stronger electron acceptor than **TPY1**. Despite **TPY1**'s weaker electron accepting ability, **TR1** is selectively formed in CD_3CN over **LR1** (6.7 : 1), suggesting that there are other driving forces than electrostatic interaction that account for **TPY**'s better templating efficiency over **BPY** in a polar solvent. The weaker electrostatic interaction in **TR1** is also supported by its solid-state structure, in which the most electron deficient parts of **TPY**, *i.e.* pyridinium units, have barely any π-overlap with the **TIP** units.

(3) The sizes and charges of π-surfaces are different. The cationic pyridinium unit is better solvated in more polar solvent such as MeCN. **BPY1** contains two pyridinium units while **TPY1** has a larger π-surface with three pyridinium units and one neutral central phenylene ring. In less polar $CDCl_3$, **TPY1** experiences significant aggregation due to poor solvation of the charged π-surface. In more polar CD_3CN, the interlocked structure is favored by situating the **TPY** core inside the cavity of the macrobicyclic cage with three pyridinium units sticking out, and the central phenylene ring overlapping with the two **TIP** π-surfaces. This geometry ensures both sufficient solvation of the cationic pyridinium units and effective shielding of the central phenylene unit to preserve the buried hydrophobic surface area from unfavorable interactions with polar solvent. The formation of a 1 : 2 complex in the solid-state structure of **TR2** is probably also driven by such a solvation effect.

Overall, the **BPY** templated assembly of linear [2]rotaxanes is driven by a combination of hydrogen bonding interactions and complementary electrostatics but not so much by

solvophobic interactions. In the cases of **TPY** templated assembly of triply threaded [2]rotaxanes, the complexation is driven by a combination of hydrogen bonding and solvophobic interactions, but not much by complementary electrostatics. It is the difference in collective non-covalent interactions that accounts for the opposite selectivity in different solvents.

Conclusions

In summary, we have demonstrated the solvent switchable formation of two dynamic [2]rotaxanes when two π cationic guests are employed. The solvent-dependent selectivity relies on the subtle differences of the aromatic–aromatic interactions that govern the templated formation of two [2]rotaxanes. The **BPY**-based clipping reaction is driven by electrostatic interactions between aromatic surfaces, while the **TPY**-based reaction is driven by solvophobic interactions. In competition clipping experiments employing both **BPY** and **TPY** as the templates, exclusive formation of the **BPY**-based linear [2]rotaxane can be achieved in pure $CDCl_3$, while in pure CD_3CN, a 8 : 1 selectivity is achieved with the **TPY**-based triply threaded [2]rotaxane as the major product. Combining the structural features of the two [2]rotaxanes and the high solvent-dependent selectivity provides a unique test bed for probing the nature of aromatic–aromatic interactions, which can be essential for the design of complex molecular architectures that greatly rely on weak but cooperative non-covalent interactions.

Acknowledgements

This study was performed at the Molecular Foundry and Advanced Light Source, Lawrence Berkeley National Laboratory, supported by the Office of Science, Office of Basic Energy Sciences, Scientific User Facilities Division, of the U.S. Department of Energy under contract no. DE-AC02-05CH11231.

Notes and references

1 (*a*) G. Barin, A. Coskun, M. M. G. Fouda and J. F. Stoddart, *ChemPlusChem*, 2012, **77**, 159–185; (*b*) C. J. Bruns and J. F. Stoddart, *Top. Curr. Chem.*, 2012, **323**, 19–72.

2 (*a*) Y. Luo, C. P. Collier, J. O. Jeppesen, K. A. Nielsen, E. DeIonno, G. Ho, J. Perkins, H. R. Tseng, T. Yamamoto, J. F. Stoddart and J. R. Heath, *ChemPhysChem*, 2002, **3**, 519–525; (*b*) S. A. Vignon, T. Jarrosson, T. Iijima, H. R. Tseng, J. K. M. Sanders and J. F. Stoddart, *J. Am. Chem. Soc.*, 2004, **126**, 9884–9885; (*c*) J. Berna, D. A. Leigh, M. Lubomska, S. M. Mendoza, E. M. Perez, P. Rudolf, G. Teobaldi and F. Zerbetto, *Nat. Mater.*, 2005, **4**, 704–710; (*d*) D. A. Leigh, M. A. F. Morales, E. M. Perez, J. K. Y. Wong, C. G. Saiz, A. M. Z. Slawin, A. J. Carmichael, D. M. Haddleton, A. M. Brouwer, W. J. Buma, G. W. H. Wurpel, S. Leon and F. Zerbetto, *Angew. Chem., Int. Ed.*, 2005, **44**, 3062–3067; (*e*) T. D. Nguyen, Y. Liu, S. Saha, K. C. F. Leung, J. F. Stoddart and J. I. Zink, *J. Am. Chem. Soc.*, 2007, **129**, 626–634; (*f*) V. Serreli, C.-F. Lee, E. R. Kay and D. A. Leigh, *Nature*, 2007, **445**, 523–527; (*g*) E. Coronado, P. Gavina and S. Tatay, *Chem. Soc. Rev.*, 2009, **38**, 1674–1689; (*h*) F. Durola, J. Lux and J.-P. Sauvage, *Chem.–Eur. J.*, 2009, **15**, 4124–4134; (*i*) S. Silvi, M. Venturi and A. Credi, *J. Mater. Chem.*, 2009, **19**, 2279–2294; (*j*) Y. Jiang, J.-B. Guo and C.-F. Chen, *Org. Lett.*, 2010, **12**, 4248–4251; (*k*) C.-F. Chen, *Chem. Commun.*, 2011, **47**, 1674–1688; (*l*) S.-Z. Hu and C.-F. Chen, *Chem.–Eur. J.*, 2011, **17**, 5424–5431.

3 (*a*) K. Kim, *Chem. Soc. Rev.*, 2002, **31**, 96–107; (*b*) V. Sindelar, S. Silvi and A. E. Kaifer, *Chem. Commun.*, 2006, 2185–2187; (*c*) F. Huang, D. S. Nagvekar, X. Zhou and H. W. Gibson, *Macromolecules*, 2007, **40**, 3561–3567; (*d*) F. Wang, C. Han, C. He, Q. Zhou, J. Zhang, C. Wang, N. Li and F. Huang, *J. Am. Chem. Soc.*, 2008, **130**, 11254–11255; (*e*) H. Zhang, Q. Wang, M. Liu, X. Ma and H. Tian, *Org. Lett.*, 2009, **11**, 3234–3237; (*f*) F. Wang, J. Zhang, X. Ding, S. Dong, M. Liu, B. Zheng, S. Li, L. Wu, Y. Yu, H. W. Gibson and F. Huang, *Angew. Chem., Int. Ed.*, 2010, **49**, 1090–1094; (*g*) S. Dong, Y. Luo, X. Yan, B. Zheng, X. Ding, Y. Yu, Z. Ma, Q. Zhao and F. Huang, *Angew. Chem., Int. Ed.*, 2011, **50**, 1905–1909; (*h*) Z. Niu, F. Huang and H. W. Gibson, *J. Am. Chem. Soc.*, 2011, **133**, 2836–2839; (*i*) Z. Zhang, Y. Luo, J. Chen, S. Dong, Y. Yu, Z. Ma and F. Huang, *Angew. Chem., Int. Ed.*, 2011, **50**, 1397–1401; (*j*) S. Dong, X. Yan, B. Zheng, J. Chen, X. Ding, Y. Yu, D. Xu, M. Zhang and F. Huang, *Chem.–Eur. J.*, 2012, **18**, 4195–4199; (*k*) X. Yan, D. Xu, X. Chi, J. Chen, S. Dong, X. Ding, Y. Yu and F. Huang, *Adv. Mater.*, 2012, **24**, 362–369; (*l*) B. Zheng, F. Wang, S. Dong and F. Huang, *Chem. Soc. Rev.*, 2012, **41**, 1621–1636.

4 (*a*) P. N. Taylor, M. J. O'Connell, L. A. McNeill, M. J. Hall, R. T. Aplin and H. L. Anderson, *Angew. Chem., Int. Ed.*, 2000, **39**, 3456–3460; (*b*) H. W. Gibson, Z. Ge, F. Huang, J. W. Jones, H. Lefebvre, M. J. Vergne and D. M. Hercules, *Macromolecules*, 2005, **38**, 2626–2637; (*c*) Y. Jiang, J. Wu, L. He, C. Tu, X. Zhu, Q. Chen, Y. Yao and D. Yan, *Chem. Commun.*, 2008, 6351–6353; (*d*) Q. Li, W. Zhang, O. S. Miljanic, C.-H. Sue, Y.-L. Zhao, L. Liu, C. B. Knobler, J. F. Stoddart and O. M. Yaghi, *Science*, 2009, **325**, 855–859; (*e*) C. Travelet, P. Hebraud, C. Perry, C. Brochon, G. Hadziioannou, A. Lapp and G. Schlatter, *Macromolecules*, 2010, **43**, 1915–1921; (*f*) N. Momcilovic, P. G. Clark, A. J. Boydston and R. H. Grubbs, *J. Am. Chem. Soc.*, 2011, **133**, 19087–19089; (*g*) A. Coskun, M. Hmadeh, G. Barin, F. Gandara, Q. Li, E. Choi, N. L. Strutt, D. B. Cordes, A. M. Z. Slawin, J. F. Stoddart, J.-P. Sauvage and O. M. Yaghi, *Angew. Chem., Int. Ed.*, 2012, **51**, 2160–2163; (*h*) M. Zhang, D. Xu, X. Yan, J. Chen, S. Dong, B. Zheng and F. Huang, *Angew. Chem., Int. Ed.*, 2012, **51**, 7011–7015.

5 (*a*) T. J. Huang, B. Brough, C. M. Ho, Y. Liu, A. H. Flood, P. A. Bonvallet, H. R. Tseng, J. F. Stoddart, M. Baller and S. Magonov, *Appl. Phys. Lett.*, 2004, **85**, 5391–5393;

(*b*) Y. Liu, A. Flood, R. Moskowitz and J. Stoddart, *Chem.–Eur. J.*, 2005, **11**, 369–385; (*c*) B. K. Juluri, A. S. Kumar, Y. Liu, T. Ye, Y.-W. Yang, A. H. Flood, L. Fang, J. F. Stoddart, P. S. Weiss and T. J. Huang, *ACS Nano*, 2009, **3**, 291–300.

6 (*a*) E. W. Wong, C. P. Collier, M. Behloradsky, F. M. Raymo, J. F. Stoddart and J. R. Heath, *J. Am. Chem. Soc.*, 2000, **122**, 5831–5840; (*b*) C. P. Collier, J. O. Jeppesen, Y. Luo, J. Perkins, E. W. Wong, J. R. Heath and J. F. Stoddart, *J. Am. Chem. Soc.*, 2001, **123**, 12632–12641; (*c*) A. R. Pease, J. O. Jeppesen, J. F. Stoddart, Y. Luo, C. P. Collier and J. R. Heath, *Acc. Chem. Res.*, 2001, **34**, 433–444; (*d*) A. H. Flood, J. F. Stoddart, D. W. Steuerman and J. R. Heath, *Science*, 2004, **306**, 2055–2056; (*e*) J. W. Choi, A. H. Flood, D. W. Steuerman, S. Nygaard, A. B. Braunschweig, N. N. P. Moonen, B. W. Laursen, Y. Luo, E. DeIonno, A. J. Peters, J. O. Jeppesen, K. Xu, J. F. Stoddart and J. R. Heath, *Chem.–Eur. J.*, 2005, **12**, 261–279; (*f*) J. E. Green, J. W. Choi, A. Boukai, Y. Bunimovich, E. Johnston-Halperin, E. DeIonno, Y. Luo, B. A. Sheriff, K. Xu, Y. S. Shin, H.-R. Tseng, J. F. Stoddart and J. R. Heath, *Nature*, 2007, **445**, 414–417; (*g*) W. Zhang, E. DeIonno, W. R. Dichtel, L. Fang, A. Trabolsi, J.-C. Olsen, D. Benitez, J. R. Heath and J. F. Stoddart, *J. Mater. Chem.*, 2011, **21**, 1487–1495.

7 (*a*) R. Hernandez, H.-R. Tseng, J. W. Wong, J. F. Stoddart and J. I. Zink, *J. Am. Chem. Soc.*, 2004, **126**, 3370–3371; (*b*) T. D. Nguyen, H.-R. Tseng, P. C. Celestre, A. H. Flood, Y. Liu, J. F. Stoddart and J. I. Zink, *Proc. Natl. Acad. Sci. U. S. A.*, 2005, **102**, 10029–10034; (*c*) S. Angelos, E. Johansson, J. F. Stoddart and J. I. Zink, *Adv. Funct. Mater.*, 2007, **17**, 2261–2271; (*d*) T. D. Nguyen, Y. Liu, S. Saha, K. C. F. Leung, J. F. Stoddart and J. I. Zink, *J. Am. Chem. Soc.*, 2007, **129**, 626–634; (*e*) S. Angelos, Y.-W. Yang, K. Patel, J. F. Stoddart and J. I. Zink, *Angew. Chem., Int. Ed.*, 2008, **47**, 2222–2226; (*f*) H. Meng, M. Xue, T. Xia, Y.-L. Zhao, F. Tamanoi, J. F. Stoddart, J. I. Zink and A. E. Nel, *J. Am. Chem. Soc.*, 2010, **132**, 12690–12697.

8 (*a*) P. L. Anelli, P. R. Ashton, R. Ballardini, V. Balzani, M. Delgado, M. T. Gandolfi, T. T. Goodnow, A. E. Kaifer, D. Philp, M. Pietraszkiewicz, L. Prodi, M. V. Reddington, A. M. Z. Slawin, N. Spencer, J. F. Stoddart, C. Vicent and D. J. Williams, *J. Am. Chem. Soc.*, 1992, **114**, 193–218; (*b*) J. Berna, G. Bottari, D. A. Leigh and E. M. Perez, *Pure Appl. Chem.*, 2007, **79**, 39–54.

9 (*a*) S. J. Rowan, S. J. Cantrill, G. R. L. Cousins, J. K. M. Sanders and J. F. Stoddart, *Angew. Chem., Int. Ed.*, 2002, **41**, 898–952; (*b*) P. T. Corbett, J. Leclaire, L. Vial, K. R. West, J.-L. Wietor, J. K. M. Sanders and S. Otto, *Chem. Rev.*, 2006, **106**, 3652–3711; (*c*) B. H. Northrop, F. Arico, N. Tangchiavang, J. D. Badjic and J. F. Stoddart, *Org. Lett.*, 2006, **8**, 3899–3902; (*d*) C. D. Meyer, C. S. Joiner and J. F. Stoddart, *Chem. Soc. Rev.*, 2007, **36**, 1705–1723; (*e*) M. E. Belowich and J. F. Stoddart, *Chem. Soc. Rev.*, 2012, **41**, 2003–2024; (*f*) Y. Liu and Z.-T. Li, *Aust. J. Chem.*, 2013, **66**, 9–22.

10 (*a*) O. Francesconi, A. Ienco, G. Moneti, C. Nativi and S. Roelens, *Angew. Chem., Int. Ed.*, 2006, **45**, 6693–6696; (*b*) X. Liu, Y. Liu, G. Li and R. Warmuth, *Angew. Chem., Int. Ed.*, 2006, **45**, 901–904; (*c*) X. Liu and R. Warmuth, *J. Am. Chem. Soc.*, 2006, **128**, 14120–14127; (*d*) J. Luo, T. Lei, X. Xu, F.-M. Li, Y. Ma, K. Wu and J. Pei, *Chem.–Eur. J.*, 2008, **14**, 3860–3865; (*e*) D. Xu and R. Warmuth, *J. Am. Chem. Soc.*, 2008, **130**, 7520–7521; (*f*) T. Tozawa, J. T. A. Jones, S. I. Swamy, S. Jiang, D. J. Adams, S. Shakespeare, R. Clowes, D. Bradshaw, T. Hasell, S. Y. Chong, C. Tang, S. Thompson, J. Parker, A. Trewin, J. Bacsa, A. M. Z. Slawin, A. Steiner and A. I. Cooper, *Nat. Mater.*, 2009, **8**, 973–978; (*g*) X.-N. Xu, L. Wang and Z.-T. Li, *Chem. Commun.*, 2009, 6634–6636; (*h*) X.-N. Xu, L. Wang, G.-T. Wang, J.-B. Lin, G.-Y. Li, X.-K. Jiang and Z.-T. Li, *Chem.–Eur. J.*, 2009, **15**, 5763–5774; (*i*) R. A. Bilbeisi, J. K. Clegg, N. Elgrishi, X. d. Hatten, M. Devillard, B. Breiner, P. Mal and J. R. Nitschke, *J. Am. Chem. Soc.*, 2011, **134**, 5110–5119; (*j*) A. Granzhan, C. M. Schouwey, T. Riis-Johannessen, R. Scopelliti and K. Severin, *J. Am. Chem. Soc.*, 2011, **133**, 7106–7115; (*k*) Y. Jin, B. A. Voss, A. Jin, H. Long, R. D. Noble and W. Zhang, *J. Am. Chem. Soc.*, 2011, **133**, 6650–6658; (*l*) J. Sun, J. L. Bennett, T. J. Emge and R. Warmuth, *J. Am. Chem. Soc.*, 2011, **133**, 3268–3271; (*m*) P. P. Neelakandan, A. Jimenez and J. R. Nitschke, *Chem. Sci.*, 2014, DOI: 10.1039/C3SC53172D. Q4

11 (*a*) K. S. Chichak, S. J. Cantrill, A. R. Pease, S. H. Chiu, G. W. V. Cave, J. L. Atwood and J. F. Stoddart, *Science*, 2004, **304**, 1308–1312; (*b*) C. D. Meyer, R. S. Forgan, K. S. Chichak, A. J. Peters, N. Tangchaivang, G. W. V. Cave, S. I. Khan, S. J. Cantrill and J. F. Stoddart, *Chem.–Eur. J.*, 2010, **16**, 12570–12581.

12 A. R. Williams, B. H. Northrop, T. Chang, J. F. Stoddart, A. J. P. White and D. J. Williams, *Angew. Chem., Int. Ed.*, 2006, **45**, 6665–6669.

13 (*a*) T. Hasell, X. F. Wu, J. T. A. Jones, J. Bacsa, A. Steiner, T. Mitra, A. Trewin, D. J. Adams and A. I. Cooper, *Nat. Chem.*, 2010, **2**, 750–755; (*b*) G. Koshkakaryan, D. Cao, L. M. Klivansky, S. J. Teat, J. L. Tran and Y. Liu, *Org. Lett.*, 2010, **12**, 1528–1531; (*c*) S. P. Black, A. R. Stefankiewicz, M. M. J. Smulders, D. Sattler, C. A. Schalley, J. R. Nitschke and J. K. M. Sanders, *Angew. Chem., Int. Ed.*, 2013, **52**, 5749–5752; (*d*) S.-T. Tung, C.-C. Lai, Y.-H. Liu, S.-M. Peng and S.-H. Chiu, *Angew. Chem., Int. Ed.*, 2013, **52**, 13269–13272.

14 (*a*) P. T. Glink, A. I. Oliva, J. F. Stoddart, A. J. P. White and D. J. Williams, *Angew. Chem., Int. Ed.*, 2001, **40**, 1870–1875; (*b*) J. Wu, K. C.-F. Leung and J. F. Stoddart, *Proc. Natl. Acad. Sci. U. S. A.*, 2007, **104**, 17266–17271; (*c*) L. M. Klivansky, G. Koshkakaryan, D. Cao and Y. Liu, *Angew. Chem., Int. Ed.*, 2009, **48**, 4185–4189; (*d*) J. Yin, S. Dasgupta and J. Wu, *Org. Lett.*, 2010, **12**, 1712–1715; (*e*) S. Dasgupta and J. Wu, *Org. Biomol. Chem.*, 2011, **9**, 3504–3515; (*f*) M. E. Belowich, C. Valente, R. A. Smaldone, D. C. Friedman, J. Thiel, L. Cronin and J. F. Stoddart, *J. Am. Chem. Soc.*, 2012, **134**,

5243–5261; (*g*) A. Pun, D. A. Hanifi, G. Kiel, E. O'Brien and Y. Liu, *Angew. Chem., Int. Ed.*, 2012, **51**, 13119–13122; (*h*) J. Li, P. Wei, X. Wu, M. Xue, X. Yan and Q. Zhou, *RSC Adv.*, 2013, **3**, 21289–21293.

15 A. Sørensen, A. M. Castilla, T. K. Ronson, M. Pittelkow and J. R. Nitschke, *Angew. Chem., Int. Ed.*, 2013, **52**, 11273–11277.

16 (*a*) S. J. Loeb, J. Tiburcio and S. J. Vella, *Chem. Commun.*, 2006, 1598–1600; (*b*) N. D. Suhan, L. Allen, M. T. Gharib, E. Viljoen, S. J. Vella and S. J. Loeb, *Chem. Commun.*, 2011, **47**, 5991–5993; (*c*) C. Wang, D. Cao, A. C. Fahrenbach, L. Fang, M. A. Olson, D. C. Friedman, S. Basu, S. K. Dey, Y. Y. Botros and J. F. Stoddart, *J. Phys. Org. Chem.*, 2012, **25**, 544–552; (*d*) M. R. Panman, B. H. Bakker, D. den Uyl, E. R. Kay, D. A. Leigh, W. J. Buma, A. M. Brouwer, J. A. J. Geenevasen and S. Woutersen, *Nat. Chem.*, 2013, **5**, 929–934.

17 S. Zarra, J. K. Clegg and J. R. Nitschke, *Angew. Chem., Int. Ed.*, 2013, **52**, 4837–4840.

18 Single crystals are grown by diffusing diethyl ether into the solution of **LR2** (in CD_3CN–MeOD) and **TR2** (in CD_3CN–$CDCl_3$).

19 The same structure has been reported previously. The data reported here are acquired on a new set of crystals and refined separately.

20 (*a*) C. A. Hunter and J. K. M. Sanders, *J. Am. Chem. Soc.*, 1990, **112**, 5525–5534; (*b*) L. M. Salonen, M. Ellermann and F. Diederich, *Angew. Chem., Int. Ed.*, 2011, **50**, 4808–4842; (*c*) C. R. Martinez and B. L. Iverson, *Chem. Sci.*, 2012, **3**, 2191–2201.